Comprehensive analysis of mitochondrial permeability transition pore activity in living cells using fluorescence-imaging-based techniques

Massimo Bonora[1,3], Claudia Morganti[1,3], Giampaolo Morciano[1,3], Carlotta Giorgi[1], Mariusz R Wieckowski[2] & Paolo Pinton[1]

[1]Department of Morphology, Surgery and Experimental Medicine, Section of Pathology, Oncology and Experimental Biology, Laboratory for Technologies of Advanced Therapies (LTTA), University of Ferrara, Ferrara, Italy. [2]Department of Biochemistry, Nencki Institute of Experimental Biology, Warsaw, Poland. [3]These authors contributed equally to this work. Correspondence should be addressed to P.P. (pnp@unife.it).

Published online 12 May 2016; doi:10.1038/nprot.2016.064

Mitochondrial permeability transition (mPT) refers to a sudden increase in the permeability of the inner mitochondrial membrane. Long-term studies of mPT revealed that this phenomenon has a critical role in multiple pathophysiological processes. mPT is mediated by the opening of a complex termed the mPT pore (mPTP), which is responsible for the osmotic influx of water into the mitochondrial matrix, resulting in swelling of mitochondria and dissipation of the mitochondrial membrane potential. Here we provide three independent optimized protocols for monitoring mPT in living cells: (i) measurement using a calcein–cobalt technique, (ii) measurement of the mPTP-dependent alteration of the mitochondrial membrane potential, and (iii) measurement of mitochondrial swelling. These procedures can easily be modified and adapted to different cell types. Cell culture and preparation of the samples are estimated to take ~1 d for methods (i) and (ii), and ~3 d for method (iii). The entire experiment, including analyses, takes ~2 h.

INTRODUCTION

mPT is believed to occur as a result of the opening of a nonspecific high-conductance channel in the inner mitochondrial membrane, which has become known as the mPTP. The mPTP may exist in low- and high-conductance modes[1]. Its low-conductance state is characterized by very limited permeability (cutoff, <300 Da), which permits the diffusion of small ions such as H^+, Ca^{2+}, and K^+ but does not trigger detectable mitochondrial swelling. Alternatively, its high-conductance state (1–1.3 nS) allows the free movement of molecules with a molecular mass up to 1.5 kDa across the inner mitochondrial membrane and results in mitochondrial matrix swelling[2].

Accumulating evidence supports the speculation that the mPTP is related to mitochondrial ATP synthase[3–7]. Our hypothesis, which was validated using the protocol described herein, indicates that a key element of the mPTP core is the c-subunit of mitochondrial ATP synthase[8,9]. This conclusion was further supported by the observations of other groups[10,11]. Interestingly, this model does not exclude the dependence and regulation of mPT by regulatory proteins previously associated with the mPTP.

Advantages and disadvantages of monitoring mPT in isolated mitochondria or intact cells

Numerous methods are available to monitor mPTP opening, which enables the study of various aspects of mPT in either isolated mitochondria or intact cells. The most popular mPT monitoring method using isolated mitochondria is based on measuring an increase in mitochondrial matrix volume with a mitochondrial swelling assay (usually detecting changes in the diffraction/absorption of light measured at 540 nm)[12,13]. mPTP opening can also be measured indirectly as, for example, the dissipation of mitochondrial membrane potential ($\Delta\psi m$)[8,14,15], elevated mitochondrial oxygen consumption (increased respiration)[16], and the capture of radioactive compounds (such as C^{14}-sucrose) in the mitochondrial matrix[17] in response to activators of mPTP opening. Another extensively used procedure is the so-called calcium-retention capacity method[18]. This technique is based on the ability of mitochondria to accumulate Ca^{2+} in the matrix ($[Ca^{2+}]_m$) before triggering mPT. To exclude mPTP-independent factors, a specific amount of Ca^{2+}, mitochondrial substrate, Pi, and adenine nucleotides has to be provided. This again implies the use of isolated mitochondria or (at least) permeabilized cells[19,20] measured by spectrofluorometry. In all cases, it is necessary to confirm that the observed changes in the aforementioned measurement parameters are directly caused by mPTP opening. For this reason, as a 'gold standard' to confirm mPT, cyclosporine A (CsA) is used to inhibit mPTP opening. CsA inhibition provides the most convincing evidence for mPT occurrence, as described in the literature. mPTP opening can also be monitored *in vivo* using radioactive deoxyglucose[21]. However, for estimation of the entrance of this compound into the mitochondrial matrix, isolation of mitochondria or at least plasma membrane permeabilization should be performed to eliminate the accumulation of radioactivity in the cytosol. This method has been used successfully to monitor mPTP opening during ischemia/reperfusion of the heart[22].

As described in detail in the present paper, assays of mPTP opening can be performed in living cells. These techniques avoid many of the artifacts (nonphysiological conditions) that accompany experiments using isolated mitochondria, and they offer the advantage of increased physiological relevance.

Overview of the protocol

mPT is a fascinating but quite obscure phenomenon that requires careful investigation in living cells. For this reason, we describe three different methods that can be used to monitor mPTP activity: the Co^{2+}–calcein assay, mitochondrial membrane depolarization, and the swelling technique.

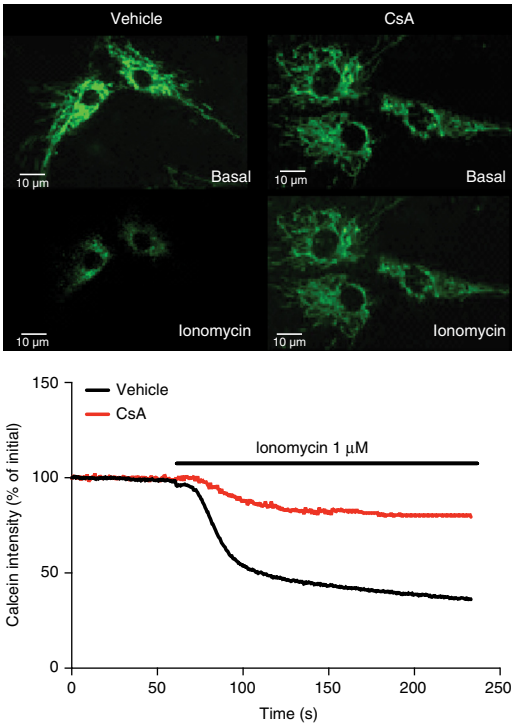

Figure 1 | Representative images and kinetics of HeLa cells stained using the Co^{2+}–calcein technique. Challenging cells with the ionophore ionomycin induced mPTP opening and quenching of the calcein signal. This event was inhibited by pretreatment with the mPTP-desensitizing agent CsA.

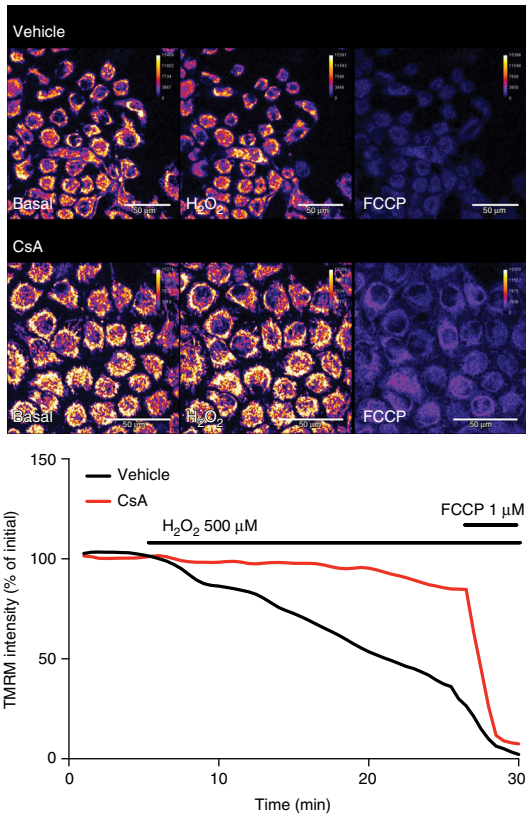

Figure 2 | Representative images and kinetics of HeLa cells stained with TMRM (Fire LUT was applied). Challenging the cells with the pro-oxidant H_2O_2 induced mPTP opening, mitochondrial depolarization, and reduced TMRM signal intensity. This was inhibited by pretreatment with the mPTP-desensitizing agent CsA. Scale bars, 50 µm.

The Co^{2+}–calcein assay is a direct and efficient method for measuring mPTP opening in living cells that has been in use since the 1990s. This method can be used in a wide range of cell types and under many pathological conditions related to the mitochondria[8,23–26]. Cells are loaded with calcein dye (excitation/emmission: 494/517 nm), which can passively diffuse into the cells and collect in cytosolic compartments including the mitochondria. Once the dye is inside cells, esterases cleave the acetoxymethyl esters, trapping the dye in intracellular compartments. At this point, the living cells become fluorescently labeled, with fluorescence spread throughout all subcellular compartments. The utility of the method originates from the ability of cobalt to quench calcein fluorescence in the cytosol but not in mitochondria. Thus, in the case of healthy cells, calcein is able to reveal the mitochondrial matrix network with good localization (**Fig. 1**). Opening of the mPTP leads to both the exit of calcein from the mitochondrial matrix and entry of Co^{2+} into the mitochondrial matrix, resulting in quenching of calcein stored in the mitochondria. This event manifests as a reduction of calcein fluorescence intensity and is easily measurable by fluorescence microscopy[27].

As mPTP opening leads to the loss of the proton gradient across membranes, the second assay measures this gradient using the Nernstian dye tetramethylrhodamine methyl ester (TMRM). TMRM is a cell-permeable, cationic, red-orange fluorescent dye. TMRM freely passes through cellular and mitochondrial membranes and, because of the large electrochemical H^+ gradient across the mitochondrial inner membrane, accumulates in the mitochondrial matrix according to $\Delta\psi m$. Opening of mPTP causes an efflux of TMRM from the mitochondria that manifests as a reduction of fluorescence intensity that is easily measurable by fluorescence microscopy (**Fig. 2**).

The final assay to verify mPTP activity is the measurement of mitochondrial network integrity. Osmotic shock induced by mPTP opening allows for the uptake of H_2O into the mitochondrial matrix and concomitant swelling of the inner mitochondrial membrane. This swelling causes mitochondria matrix expansion, which results in rupture of the outer mitochondrial membrane with loss of mitochondrial network integrity[28–30]. Overall *in vivo* mitochondrial swelling appears as a transformation of the mitochondrial network to a disorganized group of sphere-shaped structures. This can be quantified by counting the amount of objects composing the mitochondrial network when mitochondria are stained with specific fluorescent probes[8,31–33] (**Fig. 3**).

The procedure can be divided into four main and distinct sections. In the first section, seeded cells are stained to properly label mitochondria depending on the assay of interest (e.g., Co^{2+}–calcein quenching, mitochondrial depolarization, or swelling). In the second step, it is essential to set up the imaging protocol to perform basal acquisitions that are necessary before treatment with chemical compounds to modulate inhibition or induction of the mPTP. Third, challenging the mPTP opening is the aim of the protocol, so a Ca^{2+}- or reactive oxygen species (ROS)-dependent stimulus is added to the ongoing experiment. Finally, image processing and data analysis are performed to obtain a numeric index that describes mPTP activity and can be used for statistical data analysis.

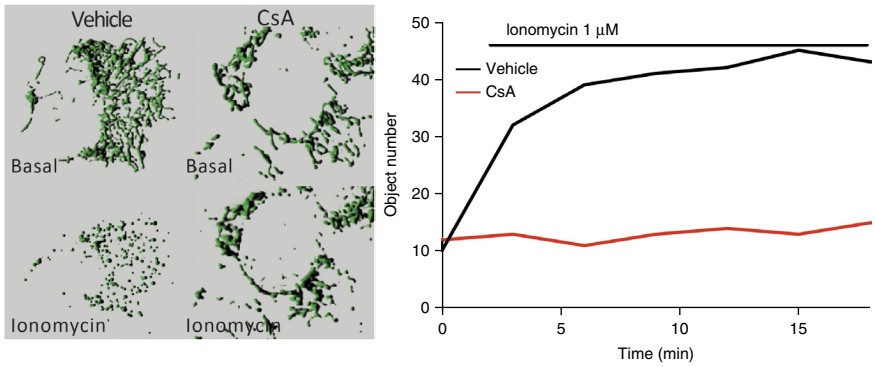

Figure 3 | Representative images and kinetics of HeLa cells expressing mitochondrially targeted GFP. Challenging the cells with the ionophore ionomycin induced mPTP opening, mitochondrial swelling, and mitochondrial network fragmentation, as represented by the increase in object count. This was inhibited by pretreatment with the mPTP-desensitizing agent CsA.

Potential applications of the protocol

The different methods described in this protocol can be used to measure mPTP opening in a wide range of intact cells. The use of the described fluorescent dyes, a controlled temperature, and the experimental setup allows for mitochondria to be present in their physiological environment. Under these conditions, the mPTP is regulated by the relevant mix of endogenous inhibitors and mPT activators in a manner that corresponds to *in vivo* conditions.

Two major advantages are obvious when considering the use of intact cells compared with isolated mitochondria or permeabilized cells. First, the system is much more physiological. Given that the mPTP interfaces with different signaling pathways, these protocols allow investigations of signaling pathways afferent to the mPTP, putative mPTP components or regulators, or novel stimulators or inhibitors of the mPT. This could be easily achieved by exposure to medium enriched with compounds of interest, or by the use of molecular biology tools such as siRNA, shRNA, cDNA overexpression of wild-type or mutant proteins, Cas9 knockout, and mutant knock-in, among many other approaches. Second, live-cell imaging requires far fewer cells than mitochondrial isolation procedures or spectrofluorimetric techniques, which extends the field of application to cells that are not easily cultured.

In our laboratory, this protocol has been successfully tested in HeLa cells, PC3 cells, HEK293T cells, SH-SY5Y cells, myoblasts, mouse embryonic fibroblasts, human adult fibroblasts, epithelial cells, HL-1 cells, rat neonatal cardiomyocytes, and CHO cells. Finally, these protocols are not time-consuming, the microscope setup is easy, and acquisition is fast. All methods apply different techniques to achieve the same purpose, so that a positive (or negative) result that is confirmed by all methods provides a high degree of statistical power and reproducibility.

Limitations of the protocol

The protocol is not feasible in cells cultured in suspension or for intact tissues. This is because of difficulties in focusing a stable sample in the former case and the thickness or degradation of the tissue slice in the latter. In addition, even if intact cells are best for testing these methods, the mPTP is not directly accessible to the full range of activators and mPT inhibitors mentioned above. Moreover, the presence of separate pools of adenine nucleotides and Ca^{2+}, and of other modulators in the cytoplasm and the mitochondrial matrix, should also be considered as a factor influencing mPT. Alternatively, studying mPTP function using isolated mitochondria simplifies the model and enables investigation of several plasma-membrane-impermeable compounds on mPT opening/closure, as well as direct control of the experimental environment by modulating, for example, the redox state and the concentrations of different ions.

Experimental design

Analysis of mPTP activity in living cells requires comparison of the results among the three imaging techniques described in this protocol. Each assay challenges mPTP in a specific manner to verify a particular aspect of its activity, and global interpretation and integration of the data are necessary in order for the results of the experiments to be fully understood. The protocol is divided into the following main sections: sample preparation, fluorescence measurements, and analysis.

Sample preparation. The first phase is relatively flexible, and it allows researchers to optimize the protocol to their own experimental situations with respect to the following specifications. Concerning cell

Box 1 | Alternative mitochondrial membrane potential probes

In addition to TMRM, several fluorescent lipophilic cationic dyes, such as tetramethylrhodamine ethyl (TMRE) ester, Rhodamine 123 (RH-123), 3,3′-dihexyloxacarbocyanine iodide (DiOC6(3)), and JC-1 (5,5′,6,6′-tetrachloro-1,1′,3,3′-tetraethylbenzimidazolylcarbocyanine iodide), are able to directly measure the mitochondrial membrane potential. As positively charged molecules, these dyes accumulate within mitochondria in inverse proportion to $\Delta\psi m$ according to the Nernst equation.

Different probes can be used for mPTP-induced mitochondrial depolarization; here, a brief description of each probe is provided, along with the modifications that researchers should make to the protocol.

TMRE is a cell-permeant, cationic, red-orange fluorescent dye that is readily sequestered by active mitochondria as TMRM. TMRM and TMRE are both quickly equilibrating dyes, but TMRM inhibits the electron-transport chain less, and it is recommended for this reason. TMRE application does not require modification of the protocol[63].

RH-123 is lipophilic in nature, which allows it to diffuse through the mitochondrial membrane in response to potential and concentration gradients. Mitochondrial energization induces the quenching of RH-123 fluorescence, and the rate of fluorescence decay is proportional to the mitochondrial membrane potential. The application of RH-123 is suggested for short-time-scale (min) studies to monitor rapid step changes in $\Delta\psi m$ (ref. 63).

(continued)

Box 1 | Alternative mitochondrial membrane potential probes (continued)

DiOC6(3) is a cell-permeant, green-fluorescent, lipophilic dye that, when used at low concentrations, is selective for the mitochondria of live cells. At higher concentrations, the dye may be used to stain other internal membranes, such as the endoplasmic reticulum. However, the use of DiOC6(3) is not recommended because of its higher toxicity toward mitochondrial respiration[64].

JC-1 is used as an indicator of mitochondrial potential in a variety of cell types. JC-1 exists as either a green-fluorescent monomer at depolarizing membrane potentials or a red-fluorescent aggregate at hyperpolarizing membrane potentials. The ratio of red to green fluorescence depends only on the membrane potential and not on other factors such as mitochondrial size, shape, and density, which may influence single-component fluorescence signals.

All these mitochondrial probes are differentially permeable according to their distinct molecular structure, and JC-1 is the least permeable. More specifically, whereas the monomer form of JC-1 has been reported to equilibrate on a time scale similar to that of TMRM/TMRE (~15 min), the aggregate form of the dye takes ~90 min to equilibrate[65]. For this reason, the use of TMRM is suggested for this particular protocol.

Additional reagents

- TMRE (Thermo Fisher Scientific, cat. no. T-669)
- RH-123 (Thermo Fisher Scientific, cat. no. R-302)
- DiOC6(3) (Thermo Fisher Scientific, cat. no. D-273)
- JC-1 dye (mitochondrial membrane potential probe; Thermo Fisher Scientific, cat. no. T-3168)

Additional procedures

For the use of RH-123 in place of TMRM, the following step should be performed instead of that in the original PROCEDURE:

- Step 2B(ii)—Cell staining: add RH-123 working solution (10 µM diluted in modified KRB) and incubate the cells for 20 min at 37 °C in a 5% CO_2 atmosphere.
- Anticipated results: using RH-123 to probe mPTP opening results in increased fluorescence, so pay particular attention to the interpretation of the data; the slope values are positive and increase in proportion to mPTP opening.

For the use of DiOC6 in place of TMRM, the following step should be performed instead of that in the original PROCEDURE:

- Step 2B(ii)—Cell staining: add DiOC6(3) working solution (<1 nM diluted in modified KRB) and incubate the cells for 20 min at 37 °C in a 5% CO_2 atmosphere.
- Step 3B—Imaging setup:

Menu	Settings
Excitation filter	Select the dedicated FITC filter set to detect DiOC6(3).
Experiment manager	Set the FITC wavelength to detect DiOC6(3) fluorescence.

Set the acquisition frequency as indicated for TMRM in **Table 3**.

For the use of JC-1 in place of TMRM, the following step should be performed instead of that in the original PROCEDURE:

- Step 2B(ii)—Cell staining: add JC-1 working solution (5 µM diluted in modified KRB) and incubate the cells for 30 min at 37 °C in a 5% CO_2 atmosphere. Remove the cells from the incubator and rinse them twice with 1 ml of modified KRB to remove the unbound dye; then, add 900 µl of modified KRB.
- Step 3B(iii)—Imaging setup and basal acquisition:

Menu	Settings
Excitation filter	Select the dedicated FITC filter set and the TRITC filter set to detect JC-1 fluorescence.
Experiment manager	Set the FITC and the TRITC wavelengths to detect both red and green dyes. Acquire two images (one red and one green) at the frequency indicated for TMRM in **Table 3**.

- Step 4B(ii)—Challenging mPTP opening: after H_2O_2 addition, acquire images for at least 40 min.
- Step 5B(i)—Image processing: open the two time-lapse images obtained (one for red and one for green fluorescence) in the Fiji software. Create a time-lapse ratio image using the process 'image calculator' and by dividing the intensity values for the red images by those for the green images. Then, using this time-lapse ratio image, proceed with the remaining image processing steps in the protocol.
- Step 5B(ii)—Image processing: on the FITC channel, draw an ROI; using freehand selections, encircle each mitochondrion, excluding the nucleus, and draw an ROI of a background region in an empty corner of the field.
- Step 5B(iii)—Image processing: for FITC and TRITC channels, estimate a global threshold to restrict the analysis to the pixels displaying intensity values greater than the threshold value.
  ▲ **CRITICAL STEP** Estimate the threshold on the final image of the time-lapse.
- Step 5B(iv)—Image processing: for FITC and TRITC channels, use the multimeasure tool to calculate the mean gray values limited by the threshold for the selected ROI (including the background ROI) in each time-lapse image.
- Step 5B(vii)—Image processing: normalize the values. Generate a new column representing the 'Ratio' value; for each timepoint, divide the TRITC intensity by the FITC intensity. Then divide each timepoint value by the initial value, considering the first value as 100%.
- Step 5B(viii)—Image processing: using the normalized 'Ratio' column, calculate the slope from minute 15 to minute 25, for instance, using the function 'SLOPE' in Microsoft Office Excel.

TABLE 1 | Genetically encoded fluorescent probes to visualize mitochondria.

Name	Fluorescent rotein	Excitation (nm)	Emission (nm)	Refs.	Distributor, code
Turquoise2-Mito	Turquoise2	425	475	53	Addgene plasmid, 36208
MtGFP	GFP10	488	515	47	NA
EYFP-Mito	EYFP	513	527	54	Clonetech, 6115-1
mtDsRed1	DsRed1	558	583	55	NA
mKate2-mito	mKate2	588	633	55	Evrogene, cat. no. FP187

NA, not applicable

seeding, it is necessary that cells reach 50–70% confluence as a monolayer on the day of the experiment. Indeed, excessive cell density can interfere with stimulus delivery and weaken mPTP activity, leading to misunderstanding of the phenomena. Moreover, the choice of a suitable imaging coverslip for individual imaging setups and cell lines is important; for instance, glass coverslips with a suitable coating should be chosen on the basis of the cell adhesion.

Cell staining and mitochondrial-labeling optimization should be specific for each of the three methods. We have found that problems may occur when calcein–cobalt formation is incomplete, leaving a large amount of cytoplasmic calcein visible (see TROUBLESHOOTING). This should be verified by microscopic examination of the coverslip before the acquisition procedure is started. A mitochondrial counterstain may be particularly helpful, and in this procedure we suggest the use of Mitotracker Red. The mitochondrial accumulation of Mitotracker is dependent on $\Delta\psi m$, and it can be partially quenched by calcein; indeed, this counterstaining is not intended for quantitative measurement and should not be included in the time-lapse acquisition.

For potentiometric measurements, TMRM is suggested, as it is probably one of the most common potentiometric dyes used. Nevertheless, alternative staining procedures that can lead to the same conclusion are described in **Box 1**.

Finally, the use of fluorescent reporters targeted to the mitochondrial matrix is strongly recommended for morphometric measurements because of their selective localization and resistance to photobleaching. The present procedures describe the use of mitochondrial GFP (mtGFP), but examples of alternatives that provide the same information are indicated in **Table 1**.

Fluorescence measurement. Imaging setup is the most critical step of the procedure; this protocol describes the most common problems that may occur at this step. Particular attention should be paid to the exposure time and light intensity to avoid artifacts due to, for instance, photobleaching of the fluorescent probe. A correct setup allows the user to obtain optimal basal measurements that are fundamental to later challenges to mPTP opening. A variety of different mPT-inducing stimuli can be used; here we describe the use of two stimuli, $[Ca^{2+}]_m$ (by means of the ionophore ionomycin) and ROS (by means of H_2O_2), that exert their effects in the range of seconds to tens of minutes, respectively. Nevertheless, alternative stimuli can be chosen depending on the experimental goals of the researcher; a list of potential alternatives is reported in **Table 2**. The time of sample acquisition varies depending on the stability of the reagents used, especially the probes. TMRM and mitochondrial fluorescent proteins are quite stable and can be monitored for up to 48–72 h. Conversely, calcein is somewhat rapidly extruded by the cell. In our hands, calcein signals display stable intensity for up to 46–60 min; indeed, for longer recording times, the user should set up the best conditions for the experimental situation. We also hasten to add that ionophores that can alter the plasma membrane potential[34] can lead to mPT-independent TMRM re-distribution. Even if the combined use of a dye for plasma membrane potential allows for the correction of this artifact, the induced mitochondrial Ca^{2+} uptake generates an mPTP-independent mitochondrial depolarization[35] that can produce experimental artifacts. Thus, even though several studies have successfully combined potentiometric dyes with ionophores to challenge mPTP opening, we recommend following this procedure, carefully evaluating the results, and considering different challenge methods (**Table 2**).

Induction and inhibition of the mPTP. Modulators of the mammalian mPTP can be divided into two classes: activators and inhibitors of mPT. mPT can be stimulated by several conditions and chemical compounds, such as accumulation of mitochondrial Ca^{2+} (ref. 36), ROS (superoxide) and pro-oxidative agents[37,38], oxidized thiols[39], P_i[40,41], long-chain free fatty acids[42], atractyloside[43],

TABLE 2 | Inducers of mPTP opening.

Stimulus	Ca^{2+} signaling	ROS signaling	Co^{2+}–calcein (refs.)	Ψm (refs.)	Mitochondrial swelling (refs.)
Ionomycin	X		8		8
A23187	X		27		56
H_2O_2		X	57	8	8
Thapsigargin	X	X	26	58	26
Menadione	X		59	59	60
Ceramide	X	X		61	62

mastoparan[44], and 1-(2-chlorophenyl)-*N*-methyl-*N*-(1-methylpropyl)-3-isoquinoline-carboxamide (PK11195)[45]. In turn, mPT can be inhibited by high $\Delta\psi m$; CsA; sanglifehrin A; bongkrekic acid; antamanide; 5-isothiocyanato-2-[2-(4-isothiocyanato-2-sulfophenyl)ethenyl]benzene-1-sulfonic acid; adenine nucleotides (ATP and ADP); creatine; cyclocreatine; glucose; König's polyanion; NADH; NADPH; UTP; ubiquinone; decylubiquinone; antioxidants; calcium chelators; and divalent cations such as Ba^{2+}, Mg^{2+}, Mn^{2+}, and Sr^{2+}. However, the conditions and compounds listed above can have no, or even opposing, effects on eukaryotic cells of different taxa (for further details, see ref. 46).

Data analysis. In this section, guidelines for image and data processing are comprehensively described to allow researchers who are not familiar with microscopy to perform the experiment. Specialists can optimize the analyses according to their own needs, but we recommend meticulously following the critical steps of the procedure.

Experimental controls. As described before, CsA is a well-known inhibitor of mPT, and its activity is reported to prevent mPTP opening. Hence, we suggest including CsA treatment as a negative control in each experiment.

MATERIALS

REAGENTS

- Sodium chloride (NaCl; Sigma-Aldrich, cat. no. S7653)
- Potassium chloride (KCl; Fluka, cat. no. 60128)
- Potassium phosphate monobasic (KH_2PO_4; Sigma-Aldrich, cat. no. P0662)
- Magnesium sulfate heptahydrate ($MgSO_4{\cdot}7H_2O$; Sigma-Aldrich, cat. no. M5921)
- $CaCl_2$, 1 M (Fluka, cat. no. 10043-52-4)
- Glucose (Sigma-Aldrich, cat. no. G7528)
- HEPES (Sigma-Aldrich, cat. no. H3375)
- Ionomycin calcium salt (Sigma-Aldrich, cat. no. I0634) **! CAUTION** Ionomycin can cause skin and eye irritation.
- MitoTracker Red CMXRos (Thermo Fisher Scientific, cat. no. M-7510)
- Cobalt(II) chloride hexahydrate ($CoCl_2$; Sigma-Aldrich, cat. no. 20 2185) **! CAUTION** $CoCl_2$ is dangerous for health and is potentially carcinogenic.
- Calcein, acetoxymethyl ester (Thermo Fisher Scientific, cat. no. C310)
- Sulfinpyrazone (Sigma-Aldrich, cat. no. S9509)
- DMSO (Sigma-Aldrich, cat. no. 154938)
- Sodium hydroxide (NaOH; Fluka, cat. no. 71691)
- Tetramethylrhodamine methyl ester (TMRM; Invitrogen, cat. no. T668)
- Hydrogen peroxide, 10 M (H_2O_2; Sigma-Aldrich, cat. no. H-1009)
- Carbonyl cyanide 4-(trifluoromethoxy)phenylhydrazone (FCCP; Sigma-Aldrich, cat. no. C2920)
- Milli-Q water (Millipore)
- Ethanol (Sigma-Aldrich, cat. no. 02860)
- Adherent cultured cell lines. The anticipated results described in this protocol have been obtained using HeLa cells (ATCC CCL-2). However, the procedure has been successfully tested in HeLa cells, PC3 cells, HEK293T cells, SH-SY5Y cells, myoblasts, mouse embryonic fibroblasts, human adult fibroblasts, epithelial cells, HL-1 cells, rat neonatal cardiomyocytes, and CHO cells **! CAUTION** Cell lines should be regularly checked to ensure that they are authentic and not infected with *Mycoplasma*.
- Mammalian expression plasmid containing the mitochondrially targeted fluorescent reporter. This protocol is performed using the plasmid encoding mtGFP, which was described by Rizzuto *et al.*[47]. However, equivalent results can be obtained using other mitochondrially targeted fluorescent proteins, as listed in **Table 1**.

EQUIPMENT

- Parafilm (Sigma-Aldrich, cat. no. P7793)
- 0.5-ml Microcentrifuge tubes
- Aluminum foil
- 35 mm #1.5 glass-bottom Petri dish (CellVis, cat. no. D35-14-1.5-N)
- Inverted wide-field fluorescence microscope
- Image analysis software. The procedure describes the use of FIJI (http://fiji.sc/Fiji)[48]; however, similar results can be obtained using equivalent competitors (i.e., PerkinElmer Volocity, Bitplane Imaris, 3i Slidebook, and Bioimageanalysis Icy)

REAGENT SETUP

Kreb's Ringer buffer Kreb's ringer buffer (KRB) is 135 mM NaCl, 5 mM KCl, 0.4 mM KH_2PO_4, 1 mM $MgSO_4{\cdot}7H_2O$, 20 mM HEPES, and 5.5 mM glucose, pH 7.4. Dissolve 7.89 g of NaCl, 0.373 g of KCl, 0.054 g of KH_2PO_4, 0.247 g of $MgSO_4{\cdot}7H_2O$, 4.76 g of HEPES, and 1 g of glucose in <1,000 ml of Milli-Q water. Adjust the pH to 7.4 with NaOH, and then bring the final volume to 1,000 ml. Store it at 4 °C for up to 3 d.

Modified KRB Add 0.5 ml of 1 M $CaCl_2$ to 500 ml of KRB. Store it at 4 °C for up to 3 d. ▲ **CRITICAL** This solution should be prepared in a polypropylene cylinder, as glass containers can bind Ca^{2+}, and this can produce imprecise experimental conditions.

Calcein, 1 mM stock solution Prepare 1 mM calcein stock solution by dissolving 50 µg of calcein in 50 µl of DMSO. Divide the stock solution into aliquots. This solution can be stored at 20 °C for 3 months. ▲ **CRITICAL** Avoid multiple freeze–thaw cycles, and protect the solution from light.

200 µM MitoTracker Red CMXRos stock solution Prepare 200 µM MitoTracker Red stock solution by dissolving 50 µg of MitoTracker Red CMXRos in 470 µl of DMSO. Divide the stock solution into aliquots. This solution can be stored at −20 °C for 3 months. ▲ **CRITICAL** Avoid multiple freeze–thaw cycles, and protect the solution from light.

1 M $CoCl_2$ stock solution Prepare 1 M $CoCl_2$ stock solution by dissolving 0.238 g of $CoCl_2$ in 1 ml of Milli-Q water. This solution can be stored at 4 °C for 3 months.

10 mM Sulfinpyrazone stock solution Prepare 10 mM sulfinpyrazone stock solution by dissolving 0.04 g of sulfinpyrazone in 10 ml of Milli-Q water. Divide the stock solution into aliquots. This solution can be stored at 4 °C for 6 months. ▲ **CRITICAL** Add NaOH to alkalinize the solution until the drug dissolves.

1 mM Ionomycin stock solution Dissolve 1 mg of ionomycin in 1.34 ml of DMSO. Divide the stock solution into aliquots. Store the aliquots at 20 °C for 6 months. ▲ **CRITICAL** Avoid multiple freeze–thaw cycles of the stock solution.

10 µM Ionomycin solution Dissolve 3 µl of 1 mM ionomycin stock solution in 300 µl of modified KRB. The solution can be stored on ice until use. At the end of the experiment, this solution should be discarded.

Calcein loading solution Prepare 1 ml of calcein loading solution by adding 1 µl of 1 mM calcein stock solution (final concentration: 1 µM), 1 µl of 200 µM MitoTracker Red CMXRos stock solution (final concentration: 200 nM), 2 µl of 1 M $CoCl_2$ stock solution (final concentration: 2 mM), and 20 µl of 10 mM sulfinpyrazone stock solution (final concentration: 200 µM) to 1 ml of KRB. ▲ **CRITICAL** Protect the solution from light and use it within 1 h of preparation. ▲ **CRITICAL** Sulfinpyrazone is recommended to inhibit organic anion transport, which can induce leakage of de-esterified acetoxymethyl (AM) indicators[49].

100 µM TMRM stock solution Dissolve 0.5 mg of TMRM powder in 10 ml of ethanol. We recommend splitting the solution into aliquots, wrapping the tubes with aluminum foil, and freezing the aliquots until use. The aliquots can be stored for 6 months at −20 °C.

10 mM FCCP stock solution Dissolve 0.025 g of FCCP powder in 10 ml of ethanol. We recommend splitting the solution into aliquots, wrapping the tubes with aluminum foil, and freezing the aliquots until use. The aliquots can be stored for 6 months at −20 °C.

10 µM TMRM loading solution Prepare the loading solution by adding 1 µl of 100 µM TMRM stock solution to 10 ml of modified KRB. The solution can be stored on ice until use. At the end of the experiment, this solution should be discarded. ▲ **CRITICAL** TMRM is sensitive to light, so avoid light exposure by handling this solution in a low-light environment and by wrapping the tubes in aluminum foil.

5 mM H_2O_2 solution Prepare H_2O_2 solution by adding 0.5 µl of 10 M H_2O_2 to 1 ml of TMRM loading solution. Because H_2O_2 is not stable, we recommend splitting the solution into aliquots of 100 µl each, wrapping the tubes with aluminum foil, and freezing the aliquots at −20 °C until use. At the end of the experiment, these aliquots should be discarded.

10 µM FCCP solution Prepare FCCP solution by adding 1 µl of 10 mM FCCP to 1 ml of TMRM loading solution. We recommend splitting the solution into aliquots of 100 µl, wrapping the tubes with aluminum foil, and freezing the aliquots at −20 °C until use. At the end of the experiment, these aliquots should be discarded.

EQUIPMENT SETUP

Microscope setup A motorized inverted fluorescence microscope equipped with high-numerical-aperture lenses, a fluorescein isothiocyanate (FITC)/tetramethylrhodamine isothiocyanate (TRIC) filter set, and environmental control is required to complete this procedure. In this protocol, the instrument described is provided by Olympus. However, similar performance can be achieved using imaging setups distributed by all the major brands in the field (e.g., Zeiss, Nikon, Leica, Crisel Instruments, and Intelligent Imaging Innovations (3i)) or using custom-built equipment. Essential components are as follows:

- Motorized Olympus IX81-ZDC inverted microscope. At a minimum, the microscope has to be motorized to allow 3D image acquisition. Equivalent equipment is available from competitors (e.g., Zeiss Axio Observer, Nikon Eclipse Ti-E, Leica DMi8).
- 40×/1.30-N.A. UPlanFLN oil-immersion objective or equivalent (e.g., Zeiss Plan-Apochromat 40×/1.3 Oil, Nikon CFI Plan Fluor 40× Oil, and Leica HC PL APO 40×/1.30 Oil CS2).
- 60×/1.35-N.A. UPlanFLN oil-immersion objective or equivalent (e.g., Zeiss Plan-Apochromat 63×/1.4 Oil, Nikon CFI Plan Apo Lambda 60× Oil, Leica HC PL APO 63×/1.40 Oil CS2).
- Cell MT20E xenon lamp. The use of an illuminating device equipped with a fast shutter is recommended to reduce photobleaching. Xenon- or light-emitting-diode-based light sources are suggested but are not mandatory (examples of equivalent competitors are Sutter Instruments Lambda DG-4 and EXCELITAS Technologies X-Cite).
- HAMAMATSU ORCA RG. The CCD camera should have a 6.45-µm pixel size to ensure the highest resolution, and it should be cooled to −30 °C for noise reduction (examples of equivalent competitors are Photometrics CoolSNAP HQ2 CCD and Andor Clara Interline CCD).
- Okolab environmental control. Optimal performance is obtained by fixing the temperature at 37 °C, setting the CO_2 level to 5%, and using a humidified environment. At a minimum, temperature control is mandatory (examples of equivalent competitors are provided by Bioscience Tools, Harvard Apparatus, and Warner Instruments).
- Xcellence rt software equipped with a 3D deconvolution module. The image acquisition software should be able to control the hardware and perform 3D reconstruction of point spread function (PSF)-degraded images. Examples of equivalent competitors are Universal Imaging Metamorph, Nikon NIS elements, Zeiss ZEN, and LEICA LAS X. High-performance 3D digital deconvolution can be performed by additional software such as PerkinElmer Volocity, Bitplane Imaris, 3i Slidebook, and Media Cybernetics Autoquant.

PROCEDURE

Cell preparation ● TIMING 1 h

1| Seed cells onto a circular imaging dish, and allow the cells to grow until they reach 50% confluence. The researcher must optimize the seeding density for the given cell line. After seeding cells, wait for at least 24 h.

Cell staining and mitochondrial labeling

2| The following section describes how to perform sample staining. Please proceed to option A for Co^{2+}–calcein, to option B for the TMRM method, and to option C for the mitochondrial morphology assay.

(A) *In vivo* measurement of mPTP-induced Co^{2+}–calcein quenching ● TIMING 20 min

(i) Remove the cells from the incubator, and wash them once with 1 ml of modified KRB to remove residual cellular debris and medium.

? TROUBLESHOOTING

(ii) Add 1 ml of calcein loading solution, and incubate the cells for 15 min at 37 °C in a 5% CO_2 atmosphere.

▲ **CRITICAL STEP** Calcein is sensitive to light. Avoid exposure to light by handling the staining solution in low-light conditions and by protecting the sample with aluminum foil during the incubation step.

? TROUBLESHOOTING

(iii) Remove the cells from the incubator and wash them twice with 1 ml of modified KRB to remove the unbound dye; then, add 900 µl of modified KRB.

▲ **CRITICAL STEP** Washing must be performed carefully. Avoid the use of automatic aspiration tools.

(B) *In vivo* measurement of mPTP-induced mitochondrial depolarization ● TIMING 40 min

(i) Remove cells from the incubator, and wash them once with 1 ml of modified KRB to remove residual cellular debris and medium.

? TROUBLESHOOTING

(ii) Add 900 µl of TMRM loading solution, and incubate the cells for 30 min at 37 °C in a 5% CO_2 atmosphere.

▲ **CRITICAL STEP** TMRM is sensitive to light. Avoid exposure to light by handling the solution in low-light conditions and by protecting the sample with aluminum foil during the incubation step.

? TROUBLESHOOTING

(C) Measurement of *in vivo* mPTP-induced mitochondrial swelling ● TIMING 90 min

(i) Once the cells have reached 40–60% confluence, transfect them with 1–2 µg of mitochondrially targeted GFP per coverslip (for equivalent reporters, see **Table 1**). The amount used for transfection depends on the chosen transfection method (usually 1 µg/cm^2 for liposome- or polyethylenimine-based transfection and 2 µg/cm^2 for Ca^{2+} phosphate–based transfection). After transfection, wait for 36–48 h.

▲ **CRITICAL STEP** Each researcher should choose the appropriate transfection reagent and optimize the transfection protocol for the particular cell line being used. Alternatively, a stable cell line can be created using standard protocols.

Imaging setup and basal acquisition

3| The following section describes how to set up for image acquisition. Please proceed to option A for Co^{2+}–calcein, to option B for the TMRM method, and to option C for the mitochondrial morphology assay.

(A) *In vivo* measurement of mPTP-induced Co^{2+}–calcein quenching ● TIMING 1–5 min

(i) Place the imaging coverslip inside the temperature-controlled (37 °C) microscope stage.

▲ **CRITICAL STEP** Living cells are sensitive to high and low temperatures. Be sure to maintain the temperature constant at 37 °C.

(ii) Start the Xcellence Olympus software, and select the following specifications, which provide optimal image acquisition under standard conditions:

Menu	Settings
Illumination settings	Switch on the illumination system and wait for ~10 min before starting
Excitation filter	Select the dedicated FITC or TRITC filter set to detect calcein or MitoTracker fluorescence, respectively
Camera control	Set the binning at 2 × 2
Microscope control	Select the 40× oil-immersion objective from the list
Experiment manager	Set the wavelength, the exposure time, and the lamp power according to **Table 3**

▲ **CRITICAL STEP** Avoid extended and intense excitation of the sample.

(iii) Focus on the sample and acquire a snapshot of a field containing cells that display a well-localized FITC signal in the mitochondrial compartment.

▲ **CRITICAL STEP** Calcein localization must overlap with the MitoTracker signal. Be sure to validate this result before the experiment.

? TROUBLESHOOTING

(iv) Strictly draw the regions of interest (ROIs) near the mitochondria of the selected cells for analysis of kinetic trends.

▲ **CRITICAL STEP** One ROI should always be dedicated to the background.

(v) Start image acquisition at the frequency indicated in **Table 3**, and perform basal recording for 1 min.

? TROUBLESHOOTING

(B) *In vivo* measurement of mPTP-induced mitochondrial depolarization ● TIMING 1–5 min

(i) Remove cells from the incubator.

▲ **CRITICAL STEP** Do not wash away the TMRM to avoid dye re-distribution.

(ii) Place the imaging dish inside the temperature-controlled (37 °C) microscope stage.

▲ **CRITICAL STEP** Living cells are sensitive to high and low temperatures. Be sure to maintain the temperature constant at 37 °C.

(iii) Start Xcellence Olympus software, and select the following specifications, which provide optimal image acquisition under standard conditions:

Menu	Settings
Illumination settings	Switch on the illumination system and wait for ~10 min before starting
Excitation filter	Select the dedicated Rhodamine filter set to detect TMRM fluorescence
Camera control	Set the binning at 2 × 2
Microscope control	Select the 40× oil-immersion objective from the list
Experiment manager	Set the wavelength, the exposure time, and the lamp power according to **Table 3**

▲ **CRITICAL STEP** Avoid extended and intense excitation of the sample.

(iv) Select suitable field: we recommend selecting a field that displays no more than 70% confluence of cells and that contains an empty corner.

? TROUBLESHOOTING

(v) Strictly draw the ROIs near the mitochondria of the selected cells for analysis of kinetic trends.

(vi) Start image acquisition at the frequency indicated in **Table 3**, and perform basal recording for 5 min.

? TROUBLESHOOTING

(C) Measurement of *in vivo* mPTP-induced mitochondrial swelling ● TIMING 1–5 min

(i) Remove the cells from the incubator, and extensively wash the cells with modified KRB.

(ii) Cover the cells with 900 µl of modified KRB.

TABLE 3 | Image acquisition settings.

Staining method	Excitation filter (nm)	Emission filter (nm)	Exposure time (ms)	Lamp power (%)	Time delay (ms)	Experiment duration (min)
Calcein	494	520	30	3	500	10
TMRM	549	573	80	15	1,800	30
mtGFP	488	535	50	10	3,600	10

(iii) Place the imaging coverslip inside the temperature-controlled (37 °C) microscope stage.
▲ **CRITICAL STEP** Living cells are sensitive to high and low temperatures. Be sure to maintain the temperature constant at 37 °C.

(iv) Start the Xcellence Olympus software, and select the following specifications, which provide optimal image acquisition under standard conditions:

Menu	Settings
Illumination settings	Switch on the illumination system and wait for ~10 min before starting
Excitation filter	Select the dedicated GFP filter set to detect mtGFP
Camera control	Set the binning at 1 × 1
Microscope control	Select the 60× oil-immersion objective from the list
Experiment manager	Set the wavelength, the exposure time, and the lamp power according to **Table 3**
	Set *Z* stack acquisition of 51 planes spaced at 200-nm intervals

▲ **CRITICAL STEP** Avoid extended and intense excitation of the sample.

(v) Focus on the sample and identify a field in which the cells display a well-localized mitochondrially targeted GFP signal in the mitochondrial compartment.
▲ **CRITICAL STEP** Be sure to select the central *Z* plane of the cell to enable acquisition of the entire cell volume.

(vi) Start image acquisition at the frequency indicated in **Table 3**, and perform basal recording for 3 min.

Challenging mPTP opening

4| The following section describes how to stimulate mPT during image acquisition. Please proceed to option A for Co^{2+}–calcein, to option B for the TMRM method, and to option C for the mitochondrial morphology assay.

(A) *In vivo* measurement of mPTP-induced Co^{2+}–calcein quenching ● TIMING 10 min

(i) Add 100 µl of 10 µM ionomycin solution and mix it carefully.
▲ **CRITICAL STEP** Add the solution without touching the coverslip to avoid shifting the selected field.

(ii) Perform acquisition for 9 min to ensure measurement of a response to the stimulus.
? TROUBLESHOOTING

(B) *In vivo* measurement of mPTP-induced mitochondrial depolarization ● TIMING 30 min

(i) Add 100 µl of 5 mM H_2O_2 solution and mix it carefully.
▲ **CRITICAL STEP** Add the solution without touching the coverslip to avoid shifting the selected field.

(ii) Perform acquisition for 20 min to ensure measurement of a response to the stimulus.
? TROUBLESHOOTING

(iii) Add 100 µl of 10 µM FCCP solution and mix it carefully.
▲ **CRITICAL STEP** Add the solution without touching the coverslip to avoid shifting the selected field.

(iv) Perform acquisition for 5 min to ensure measurement of a response to the stimulus.
? TROUBLESHOOTING

(C) Measurement of *in vivo* mPTP-induced mitochondrial swelling ● TIMING 10 min

(i) Add 100 µl of 10 µM ionomycin solution and mix carefully.
▲ **CRITICAL STEP** Add the solution without touching the coverslip to avoid shifting the selected field.

(ii) Perform acquisition for 15 min to ensure measurement of a response to the stimulus.
? TROUBLESHOOTING

Image processing and data analysis

5| The following section describes how to perform image correction, data extraction, and analysis. Please proceed to option A for Co^{2+}–calcein, to option B for the TMRM method, and to option C for mitochondria morphology assay.

(A) *In vivo* measurement of mPTP-induced Co^{2+}-calcein quenching ● TIMING 10 min

(i) Export the results as a spreadsheet by clicking "Save As" on the kinetic graph.

(ii) Open the exported files using spreadsheet software, and subtract the background trace from each ROI arranged in a column.

(iii) Calculate the slope of the curves for the first minute after ionomycin stimulation, for instance, using the function 'SLOPE' in Microsoft Office Excel.

(iv) Input the slope values in a single column, and proceed with statistical analysis.

▲ **CRITICAL STEP** Slope calculation for periods of >1 min may underestimate the final results.

▲ **CRITICAL STEP** See **Supplementary Video 1** for a video tutorial on this section (step 5A).

(B) *In vivo* measurement of mPTP-induced mitochondrial depolarization ● TIMING 10 min

(i) Open time-lapse image using the Fiji software.

(ii) Draw an ROI; using freehand selections, encircle each mitochondrion, excluding the nucleus, and draw an ROI of a background region in an empty corner of the field.

(iii) Estimate a global threshold to restrict the analysis to the pixels displaying intensity values greater than the threshold value.

▲ **CRITICAL STEP** Estimate the threshold on the final image of the time-lapse.

(iv) Use the multimeasure tool to calculate the mean gray values limited by the threshold for the selected ROI (including the background ROI) in each time-lapse image.

(v) Export the data in a spreadsheet-compatible format (i.e., Microsoft Office Excel) and arrange the data for each ROI in a single column.

(vi) For every column, subtract the background value at the sampling time.

(vii) Normalize the values, considering the first value as 100%.

(viii) Calculate the slope from minute 15 to minute 25, for instance, using the function 'SLOPE' in Microsoft Office Excel.

▲ **CRITICAL STEP** Every trace must be analyzed using the same parameters, especially in the time-lapse slope calculation.

(ix) Use the slope values to perform statistical analysis, and compare the results under different experimental conditions.

▲ **CRITICAL STEP** See **Supplementary Video 2** for a video tutorial on this section (step 5B).

(C) Measurement of *in vivo* mPTP-induced mitochondrial swelling ● TIMING 30 min

(i) Select the last acquired time-lapse image and apply 3D digital deconvolution. Ensure that *XY* and *Z* calibration and the refraction index of the lens are properly set. Be sure to perform automated spherical aberration detection.

(ii) Export the deconvolved time-lapse image as multiple TIFF or Image Cytometry Standard files.

(iii) Open Fiji software and load the generated files.

? TROUBLESHOOTING

(iv) Split different time points using the tool 'Stack Splitter'; set the number of substacks as the number of time points (Menu Image → Stack → Tools).

(v) Select time point 1 and open the 3D object counter tool (Menu Analyze).

(vi) Set the threshold to include all mitochondria and to exclude the background. Set the minimum object size to ten pixels to avoid noise contamination.

(vii) Record the number of objects counted.

(viii) Repeat this procedure for all time points.

(ix) Collect all object counts in a spreadsheet file, arranging the data by row or column.

▲ **CRITICAL STEP** See **Supplementary Video 3** for a video tutorial on this section (step 5C).

? TROUBLESHOOTING

? TROUBLESHOOTING

Troubleshooting advice can be found in **Table 4**.

TABLE 4 | Troubleshooting table.

Step	Problem	Possible reason	Solution
2A(i), 2B(i)	Cells detach from the coverslip	Low adhesion of cells	Prepare a selective coating (depending on the cell type)
2A(ii), 2B(ii)	Cells detach from the coverslip	Cells are lost during the staining phase	Replace KRB solution with HBSS or phenol-red-free DMEM supplemented with 10% FBS

(continued)

TABLE 4 | Troubleshooting table (continued).

Step	Problem	Possible reason	Solution
3A(iii)	Nonspecific staining	Presence of cellular debris	Increase the number of washes before and after the staining phase
	Calcein fluorescence is not localized to mitochondria	Cytosolic calcein is not quenched during basal acquisition	Increase the $CoCl_2$ concentration in the staining solution (from 1 to 2 mM)
3A(v), 3B(vi)	Progressive reduction in basal fluorescence	Fluorophore bleaching	Decrease the light source power and/or the exposure time
3B(vi)	Signal is unstable during the first 5 min	TMRM loading solution is not equilibrated because of a difference in the temperature between the incubator and the microscope stage	Keep the sample on the stage until the dye reaches equilibrium (it could take up to 30 min)
	Progressive reduction in basal fluorescence intensity	TMRM is extruded from the cells by the drug delivery system	Add 250 µM sulfinpyrazone to the loading solution
3B(iv)	Very weak signal	TMRM loading solution was washed away	Replace the TMRM loading solution
3A(iii), 3B(iv)	Very weak signal	Stock solution was exposed to light	Use a fresh aliquot of stock solution
4A(ii), 4B(ii), 4B(iv), 4C(ii)	Delayed or absent response to stimuli	Improper stimulus concentration	Increase the stimulus concentration
		Degraded stimulus solution	Prepare fresh stimulus solution
		Stimulus does not reach the selected cells	Mix the solution more extensively in the imaging chamber
		Excessive cell density hampers stimulus distribution or reduces the stimulus strength	Reduce the density of cells in the seeding phase
4A(ii), 4B(ii), 4C(ii)	Delayed or absent response to stimuli	Cells withstand mPTP opening	Elongate the length of time-lapse imaging
4A(ii)	Cytosolic fluorescence quenching is not maintained during stimulus-induced mPTP opening	Extrusion of cytosolic $CoCl_2$	Increase $CoCl_2$ concentration in the medium
5C(iii)	The 3D time-lapse acquisition appears as a single stack; there is no separation between time points	The software could not differentiate between *Z* and *t* dimensions	Manually define the *Z* and *t* dimensions (Menu Image → Hyperstack → Stack to Hyperstack)
5C(ix)	Object number progressively increases independently of mPTP challenging	Signal photobleaching causes reduction of the optimal thresholding value, with consequent artificial object fragmentation	Decrease the light source power and/or the exposure time

● TIMING

Experiment and reagent setup: ~1 week
Step 1, cell preparation: 1 h
Step 2, cell staining and mitochondrial labeling
Step 2A, *in vivo* measurement of mPTP-induced Co^{2+}-calcein quenching: 20 min
Step 2B, *in vivo* measurement of mPTP-induced mitochondrial depolarization: 40 min
Step 2C, measurement of *in vivo* mPTP-induced mitochondrial swelling: 90 min

Step 3, imaging setup and basal acquisition
Step 3A, *in vivo* measurement of mPTP-induced Co^{2+}–calcein quenching: 1–5 min
Step 3B, *in vivo* measurement of mPTP-induced mitochondrial depolarization: 1–5 min
Step 3C, measurement of *in vivo* mPTP-induced mitochondrial swelling: 1–5 min
Step 4, challenging mPTP opening
Step 4A, *in vivo* measurement of mPTP-induced Co^{2+}–calcein quenching: 10 min
Step 4B, *in vivo* measurement of mPTP-induced mitochondrial depolarization: 30 min
Step 4C, measurement of *in vivo* mPTP-induced mitochondrial swelling: 10 min
Step 5, image processing and data analysis
Step 5A, *in vivo* measurement of mPTP-induced Co^{2+}–calcein quenching: 10 min
Step 5B, *in vivo* measurement of mPTP-induced mitochondrial depolarization: 10 min
Step 5C, measurement of *in vivo* mPTP-induced mitochondrial swelling: 30 min
Box 1, alternative mitochondrial membrane potential probes: 80–85 min

ANTICIPATED RESULTS

During analysis of mPTP activity by the calcein–Co^{2+} technique, basal measurements should produce a stable signal. If the signal does not seem stable or if calcein displays a localization pattern that is different from that of MitoTracker (or another counterstain, if used), please refer to Table 4 for Troubleshooting guidelines (**Supplementary Fig. 1**).

Stimulating cells with ionomycin facilitates the entry of excess Ca^{2+} into cells to trigger mPTP opening. This event causes Co^{2+} entry into the mitochondria, thereby quenching the calcein signal. Indeed, kinetic analysis should produce a slope that adequately reflects mPTP opening. The response to ionomycin can be partially blocked using CsA, a compound that has been reported to desensitize mPTP formation by binding to cyclophilin D[50]. Thus, under this experimental condition, calcein is not quenched after mPTP challenge, and the slope of the time-dependent calcein intensity should be nearly zero (**Fig 1**).

As oxidative stress is one of the best characterized homeostatic perturbations that promotes mPTP opening[51,52], the mitochondria of cells exposed to the prototypic pro-oxidant H_2O_2 underwent rapid depolarization. As described in the PROCEDURE section, the cells were stained with TMRM, a cell-permeant, cationic, red-orange fluorescent dye that is sensitive to $\Delta\psi m$. The time-lapse images were analyzed and converted to a plot as described above. In **Figure 2**, representative images of TMRM staining under basal, H_2O_2-stimulated, and residual polarization conditions and a representative trace are reported. TMRM fluorescence was stable for the first 5 min (basal conditions). Subsequently, challenge with 500 μM H_2O_2 induced a gradual decrease in the TMRM signal due to mPTP-opening-dependent depolarization. The slope of the trace directly correlates to mPTP opening. The slope of each trace derived from single cells can be used to compare different experimental conditions (i.e., vehicle versus CsA treatment). At the end of the experiment, FCCP, a mitochondrial electron-chain-uncoupling agent, was added to induce complete mitochondrial membrane depolarization. The residual TMRM staining intensity is due to non-mitochondrial membrane potential—for instance, cellular membrane potential—which should be excluded from analysis.

Traces obtained from the analysis are suitable indexes for interpreting when an experiment is not properly set up. **Supplementary Figure 1** shows two examples of the most common artifactual results; please also refer to the Troubleshooting guidelines.

Challenging cells with ionomycin leads to the deformation of mitochondrial filaments and transforms them into groups of spheroidal objects (**Fig 3**). The number of mitochondria obtained according to the instructions in this protocol is expected to markedly increase. This mitochondrial network rearrangement is inhibited by pretreatment with the mPTP-desensitizing agent CsA. If mitochondria sense some environmental stress (i.e., excess light illumination), then undesired fragmentation might be observed before the mPTP stimulation. In the case of unfortunate events such as that described, please refer to the Troubleshooting guidelines (**Supplementary Fig. 1**).

Note: Any Supplementary Information and Source Data files are available in the online version of the paper.

ACKNOWLEDGMENTS P.P. is grateful to Camilla degli Scrovegni for continuous support. This research was supported by the Italian Ministry of Education, University and Research (COFIN no. 20129JLHSY_002, FIRB no. RBAP11FXBC_002, and Futuro in Ricerca no. RBFR10EGVP_001), local funds from the University of Ferrara and the Italian Ministry of Health to P.P. and C.G., Telethon (GGP15219/B), the Italian Association for Cancer Research (IG-14442 and MFAG-13521 to P.P. and C.G.), and the Italian Cystic Fibrosis Research Foundation (19/2014) to P.P. M.R.W. was supported by the National Science Centre, Poland (grant 2014/15/B/NZ1/00490), grant W100/HFSC/2011, and HFSP grant RGP0027/2011.

AUTHOR CONTRIBUTIONS M.B., C.M., G.M., C.G., M.R.W., and P.P. contributed extensively to the writing of this paper. M.B., G.M., and C.M. performed the experiments, analyzed data, and generated visual guides.

COMPETING FINANCIAL INTERESTS The authors declare no competing financial interests.

1. Zoratti, M. & Szabo, I. The mitochondrial permeability transition. *Biochim. Biophys. Acta* **1241**, 139–176 (1995).

2. Kwong, J.Q. & Molkentin, J.D. Physiological and pathological roles of the mitochondrial permeability transition pore in the heart. *Cell Metab.* **21**, 206–214 (2015).
3. Bernardi, P. & Di Lisa, F. The mitochondrial permeability transition pore: molecular nature and role as a target in cardioprotection. *J. Mol. Cell. Cardiol.* **78**, 100–106 (2015).
4. Bonora, M. *et al.* Molecular mechanisms of cell death: central implication of ATP synthase in mitochondrial permeability transition. *Oncogene* **34**, 1475–1486 (2015).
5. Halestrap, A.P. The C ring of the F1Fo ATP synthase forms the mitochondrial permeability transition pore: a critical appraisal. *Front. Oncol.* **4**, 234 (2014).
6. Halestrap, A.P. & Richardson, A.P. The mitochondrial permeability transition: a current perspective on its identity and role in ischaemia/reperfusion injury. *J. Mol. Cell. Cardiol.* **78**, 129–141 (2015).
7. Morciano, G. *et al.* Molecular identity of the mitochondrial permeability transition pore and its role in ischemia-reperfusion injury. *J. Mol. Cell. Cardiol.* **78**, 142–153 (2015).
8. Bonora, M. *et al.* Role of the c subunit of the FO ATP synthase in mitochondrial permeability transition. *Cell Cycle* **12**, 674–683 (2013).
9. De Marchi, E., Bonora, M., Giorgi, C. & Pinton, P. The mitochondrial permeability transition pore is a dispensable element for mitochondrial calcium efflux. *Cell Calcium* **56**, 1–13 (2014).
10. Alavian, K.N. *et al.* An uncoupling channel within the c-subunit ring of the F1FO ATP synthase is the mitochondrial permeability transition pore. *Proc. Natl. Acad. Sci. USA* **111**, 10580–10585 (2014).
11. Azarashvili, T. *et al.* Potential role of subunit c of F0F1-ATPase and subunit c of storage body in the mitochondrial permeability transition. Effect of the phosphorylation status of subunit c on pore opening. *Cell Calcium* **55**, 69–77 (2014).
12. Crofts, A.R. & Chappell, J.B. Calcium ion accumulation and volume changes of isolated liver mitochondria. Reversal of calcium ion-induced swelling. *Biochem. J.* **95**, 387–392 (1965).
13. Chappell, J.B. & Crofts, A.R. Calcium ion accumulation and volume changes of isolated liver mitochondria. Calcium ion-induced swelling. *Biochem. J.* **95**, 378–386 (1965).
14. Hausenloy, D.J., Duchen, M.R. & Yellon, D.M. Inhibiting mitochondrial permeability transition pore opening at reperfusion protects against ischaemia-reperfusion injury. *Cardiovas. Res.* **60**, 617–625 (2003).
15. Wieckowski, M.R. & Wojtczak, L. Fatty acid-induced uncoupling of oxidative phosphorylation is partly due to opening of the mitochondrial permeability transition pore. *FEBS Lett.* **423**, 339–342 (1998).
16. Gautier, C.A. *et al.* Regulation of mitochondrial permeability transition pore by PINK1. *Mol. Neurodegener.* **7**, 22 (2012).
17. Crompton, M. The mitochondrial permeability transition pore and its role in cell death. *Biochem. J.* **341**, 233–249 (1999).
18. Wong, R., Steenbergen, C. & Murphy, E. Mitochondrial permeability transition pore and calcium handling. *Methods Mol. Biol.* **810**, 235–242 (2012).
19. Marcu, R., Neeley, C.K., Karamanlidis, G. & Hawkins, B.J. Multi-parameter measurement of the permeability transition pore opening in isolated mouse heart mitochondria. *J. Vis. Exp.* **67** (2012).
20. Varanyuwatana, P. & Halestrap, A.P. The roles of phosphate and the phosphate carrier in the mitochondrial permeability transition pore. *Mitochondrion* **12**, 120–125 (2012).
21. Piwocka, K. *et al.* A novel apoptosis-like pathway, independent of mitochondria and caspases, induced by curcumin in human lymphoblastoid T (Jurkat) cells. *Exp. Cell Res.* **249**, 299–307 (1999).
22. Griffiths, E.J. & Halestrap, A.P. Mitochondrial non-specific pores remain closed during cardiac ischaemia, but open upon reperfusion. *Biochem. J.* **307**, 93–98 (1995).
23. Gillessen, T., Grasshoff, C. & Szinicz, L. *Biomed. Pharmacother.* **56**, 186–193 (2002).
24. Hausenloy, D., Wynne, A., Duchen, M. & Yellon, D. Transient mitochondrial permeability transition pore opening mediates preconditioning-induced protection. *Circulation* **109**, 1714–1717 (2004).
25. Petronilli, V. *et al.* Transient and long-lasting openings of the mitochondrial permeability transition pore can be monitored directly in intact cells by changes in mitochondrial calcein fluorescence. *Biophys. J.* **76**, 725–734 (1999).
26. Woollacott, A.J. & Simpson, P.B. High throughput fluorescence assays for the measurement of mitochondrial activity in intact human neuroblastoma cells. *J. Biomol. Screen.* **6**, 413–420 (2001).
27. Petronilli, V. *et al.* Transient and long-lasting openings of the mitochondrial permeability transition pore can be monitored directly in intact cells by changes in mitochondrial calcein fluorescence. *Biophys. J.* **76**, 725–734 (1999).
28. Feldmann, G. *et al.* Opening of the mitochondrial permeability transition pore causes matrix expansion and outer membrane rupture in Fas-mediated hepatic apoptosis in mice. *Hepatology* **31**, 674–683 (2000).
29. Wakabayashi, T. Structural changes of mitochondria related to apoptosis: swelling and megamitochondria formation. *Acta Biochim. Pol.* **46**, 223–237 (1999).
30. Kaasik, A., Safiulina, D., Zharkovsky, A. & Veksler, V. Regulation of mitochondrial matrix volume. *Am. J. Phys.* **292**, C157–C163 (2007).
31. Song, W. *et al.* Assessing mitochondrial morphology and dynamics using fluorescence wide-field microscopy and 3D image processing. *Methods* **46**, 295–303 (2008).
32. Leonard, A.P. *et al.* Quantitative analysis of mitochondrial morphology and membrane potential in living cells using high-content imaging, machine learning, and morphological binning. *Biochim. Biophys. Acta* **1853**, 348–360 (2015).
33. Reis, Y. *et al.* Multi-parametric analysis and modeling of relationships between mitochondrial morphology and apoptosis. *PLoS One* **7**, e28694 (2012).
34. Nicholls, D.G. Simultaneous monitoring of ionophore- and inhibitor-mediated plasma and mitochondrial membrane potential changes in cultured neurons. *J. Biol. Chem.* **281**, 14864–14874 (2006).
35. Loew, L.M., Carrington, W., Tuft, R.A. & Fay, F.S. Physiological cytosolic Ca2+ transients evoke concurrent mitochondrial depolarizations. *Proc. Natl. Acad. Sci. USA* **91**, 12579–12583 (1994).
36. Haworth, R.A. & Hunter, D.R. The Ca2+-induced membrane transition in mitochondria. II. Nature of the Ca2+ trigger site. *Arch. Biochem. Biophys.* **195**, 460–467 (1979).
37. Takeyama, N., Matsuo, N. & Tanaka, T. Oxidative damage to mitochondria is mediated by the Ca(2+)-dependent inner-membrane permeability transition. *Biochem. J.* **294**, 719–725 (1993).
38. Kowaltowski, A.J., Castilho, R.F. & Vercesi, A.E. Mitochondrial permeability transition and oxidative stress. *FEBS Lett.* **495**, 12–15 (2001).
39. Petronilli, V. *et al.* The voltage sensor of the mitochondrial permeability transition pore is tuned by the oxidation-reduction state of vicinal thiols. Increase of the gating potential by oxidants and its reversal by reducing agents. *J. Biol. Chem.* **269**, 16638–16642 (1994).
40. Bravo, C., Chavez, E., Rodriguez, J.S. & Moreno-Sanchez, R. The mitochondrial membrane permeability transition induced by inorganic phosphate or inorganic arsenate. A comparative study. *Comp. Biochem. Physiol. B Biochem. Mol. Biol.* **117**, 93–99 (1997).
41. Kowaltowski, A.J., Castilho, R.F. & Vercesi, A.E. Opening of the mitochondrial permeability transition pore by uncoupling or inorganic phosphate in the presence of Ca2+ is dependent on mitochondrial-generated reactive oxygen species. *FEBS Lett.* **378**, 150–152 (1996).
42. Wieckowski, M.R., Brdiczka, D. & Wojtczak, L. Long-chain fatty acids promote opening of the reconstituted mitochondrial permeability transition pore. *FEBS Lett.* **484**, 61–64 (2000).
43. Beutner, G., Ruck, A., Riede, B., Welte, W. & Brdiczka, D. Complexes between kinases, mitochondrial porin and adenylate translocator in rat brain resemble the permeability transition pore. *FEBS Lett.* **396**, 189–195 (1996).
44. Pfeiffer, D.R., Gudz, T.I., Novgorodov, S.A. & Erdahl, W.L. The peptide mastoparan is a potent facilitator of the mitochondrial permeability transition. *J. Biol. Chem.* **270**, 4923–4932 (1995).
45. Li, J., Wang, J. & Zeng, Y. Peripheral benzodiazepine receptor ligand, PK11195 induces mitochondria cytochrome c release and dissipation of mitochondria potential via induction of mitochondria permeability transition. *Eur. J. Pharmacol.* **560**, 117–122 (2007).
46. Vianello, A. *et al.* The mitochondrial permeability transition pore (PTP)-an example of multiple molecular exaptation? *Biochim. Biophys. Acta* **1817**, 2072–2086 (2012).
47. Rizzuto, R., Brini, M., Pizzo, P., Murgia, M. & Pozzan, T. Chimeric green fluorescent protein as a tool for visualizing subcellular organelles in living cells. *Curr. Biol.* **5**, 635–642 (1995).
48. Schindelin, J. *et al.* Fiji: an open-source platform for biological-image analysis. *Nat. Methods* **9**, 676–682 (2012).
49. Di Virgilio, F., Fasolato, C. & Steinberg, T.H. Inhibitors of membrane transport system for organic anions block fura-2 excretion from PC12 and N2A cells. *Biochem. J.* **256**, 959–963 (1988).
50. Crompton, M., Ellinger, H. & Costi, A. Inhibition by cyclosporin A of a Ca2+-dependent pore in heart mitochondria activated by inorganic phosphate and oxidative stress. *Biochem. J.* **255**, 357–360 (1988).
51. Baines, C.P. *et al.* Loss of cyclophilin D reveals a critical role for mitochondrial permeability transition in cell death. *Nature* **434**, 658–662 (2005).

52. Kroemer, G., Galluzzi, L. & Brenner, C. Mitochondrial membrane permeabilization in cell death. *Physiol. Rev.* **87**, 99–163 (2007).
53. Goedhart, J. *et al.* Structure-guided evolution of cyan fluorescent proteins towards a quantum yield of 93%. *Nat. Commun.* **3**, 751 (2012).
54. Sarkar, A.R. *et al.* Red emissive two-photon probe for real-time imaging of mitochondria trafficking. *Anal. Chem.* **86**, 5638–5641 (2014).
55. Morozova, K.S. *et al.* MFar-red fluorescent protein excitable with red lasers for flow cytometry and superresolution STED nanoscopy. *Biophys. J.* **99**, L13–L15 (2010).
56. Dumas, J.F. *et al.* Effect of transient and permanent permeability transition pore opening on NAD(P)H localization in intact cells. *J. Biol. Chem.* **284**, 15117–15125 (2009).
57. Bejarano, I. *et al.* Role of calcium signals on hydrogen peroxide-induced apoptosis in human myeloid HL-60 Cells. *Int. J. Biomed. Sci.* **5**, 246–256 (2009).
58. Deniaud, A. *et al.* Endoplasmic reticulum stress induces calcium-dependent permeability transition, mitochondrial outer membrane permeabilization and apoptosis. *Oncogene* **27**, 285–299 (2008).
59. Gerasimenko, J.V. *et al.* Menadione-induced apoptosis: roles of cytosolic Ca(2+) elevations and the mitochondrial permeability transition pore. *J. Cell Sci.* **115**, 485–497 (2002).
60. Loor, G. *et al.* Menadione triggers cell death through ROS-dependent mechanisms involving PARP activation without requiring apoptosis. *Free Radic. Biol. Med.* **49**, 1925–1936 (2010).
61. Novgorodov, S.A. & Gudz, T.I. Ceramide and mitochondria in ischemic brain injury. *Int. J. Biochem. Mol. Biol.* **2**, 347–361 (2011).
62. Parra, V. *et al.* Changes in mitochondrial dynamics during ceramide-induced cardiomyocyte early apoptosis. *Cardiovasc. Res.* **77**, 387–397 (2008).
63. Perry, S.W., Norman, J.P., Barbieri, J., Brown, E.B. & Gelbard, H.A. Mitochondrial membrane potential probes and the proton gradient: a practical usage guide. *Biotechniques* **50**, 98–115 (2011).
64. Salvioli, S., Ardizzoni, A., Franceschi, C. & Cossarizza, A. JC-1, but not DiOC6(3) or rhodamine 123, is a reliable fluorescent probe to assess delta psi changes in intact cells: implications for studies on mitochondrial functionality during apoptosis. *FEBS Lett.* **411**, 77–82 (1997).
65. Ohno, R., Koie, K., Kamiya, T., Kawashima, K. & Ishiguro, J. [Treatment of pulmonary infections probably caused by fungi in patients with acute leukemia with chlotrimazole (author's transl.)]. *Rinsho Ketsueki* **17**, 876–883 (1976).